The Challenges of Accurate J_{0e} Determination on Modern Solar Cells: A Sensitivity Study of Input Parameter Uncertainty

Adrienne L. Blum, Harrison W. Wilterdink, and Ronald A. Sinton

***Abstract*—Carrier recombination lifetime parameters, including effective lifetime (τ_{eff}), emitter saturation current density (J_{0e}), and bulk lifetime (τ_{bulk}) on silicon photovoltaic cells, are essential quality metrics for sample characterization and enable power loss analyses that drive process optimization decisions. The carrier recombination lifetime of cells is derived from measured Suns-Voc data based on sample-specific inputs of substrate thickness and resistivity. This work presents a sensitivity analysis of the carrier recombination lifetime measurements on silicon photovoltaic cells due to uncertainty in input thickness and resistivity and proposes best practices to reduce these uncertainties to achieve results with a high level of confidence. J_{0e} uncertainties less than 1 fA/cm^2 can be achieved with measurement or knowledge of input parameters beyond what is given on a specification sheet.**

***Index Terms*—Charge carrier density, charge carrier lifetime, Monte–Carlo methods, photovoltaic (PV) cells, silicon.**

I. Introduction

CARRIER recombination lifetime parameters, including effective lifetime (τ_{eff}), emitter saturation current density (J_{0e}), and bulk lifetime (τ_{bulk}), are key characterization parameters for process optimization and control in silicon photovoltaic (PV) cell research and production. In such applications, these parameters are critical in determining power loss mechanisms to pinpoint future process improvements [1]. With technological advancements in PV [2], J_{0e} values less than 10 fA/cm^2 are routinely achieved on many different cell designs. With the increasingly low J_{0e} values seen, reporting of the J_{0e} with less than 1 fA/cm^2 of uncertainty is a desirable objective.

Cell thickness and resistivity affect the uncertainties in the J_{0e} and other carrier recombination lifetime parameters, but they are often only known within the ranges reported on wafer specification sheets [3], [4], [5]. Tracking these substrate-specific characteristics on a per wafer basis is highly uncommon. The authors in [6], [7], and [8] demonstrated sensitivity analyses at the wafer level for eddy current-based carrier recombination lifetime measurements due to input parameter uncertainty. This work will apply a sensitivity analysis to lifetime measurements on finished cells utilizing Suns-Voc data [9].

Received 19 May 2025; revised 29 July 2025; accepted 4 August 2025. Date of publication 20 August 2025; date of current version 23 October 2025. *(Corresponding author: Adrienne L. Blum.)*

The authors are with the Sinton Instruments, Boulder, CO 80301 USA (e-mail: adrienne@sintoninstruments.com; harrison@sintoninstruments.com; ron@sintoninstruments.com).

Digital Object Identifier 10.1109/JPHOTOV.2025.3596620

Cell test is a unique step in the PV manufacturing process because it is routinely performed on 100% of cells prior to module manufacture. To maximize this opportunity, as much information should be gathered as possible about each device with standard *I–V* measurements and advanced characterization. This allows for the flow of important process optimization information back into cell manufacturing or forward into module manufacturing.

At cell test, the current density, J, voltage, V, and carrier density, Δn, in the solar cell are related through (1) by several device parameters, including thickness, W, and resistivity (or equivalently doping, $N_{A,D}$) [10]. This equation is both directly dependent on substrate doping and thickness (as shown) and also indirectly dependent on these parameters through implicit dependence of Δn, τ_{eff}, and intrinsic carrier density (n_i) on both the substrate doping and thickness. The relationship found in (1) allows for full characterization of both the electrical and recombination characteristics of a cell

$$V - R_s J = \frac{kT}{q} \ln\left[\frac{(J_{sc} - J)(N_A + \Delta n)\tau_{\text{eff}}}{qW{n_i}^2}\right]. \quad (1)$$

The τ_{eff} from (1) is corrected for Auger and radiative recombination to give $\tau_{\text{corrected}}$. When $1/\tau_{\text{corrected}}$ is plotted against $(N_{A,D} + \Delta n)/qWn_i^2$, the slope and intercept of this curve at the most highly injected and linear portion can be used to calculate J_{0e} and τ_{bulk} [11], [12]. The slope-intercept form of the equation is found in (2) with the slope being used to evaluate J_{0e} and the intercept providing the τ_{bulk} parameter. In this work, J_{0e} refers to the effective emitter saturation current density, which includes surface recombination from both the front and rear surfaces of the cell. In addition, we define τ_{bulk} as the bulk lifetime parameter that is derived from (2) that represents recombination occurring in the bulk, excluding contributions from Auger and radiative recombination mechanisms

$$\frac{1}{\tau_{\text{corrected}}} = J_{0e}\left(\frac{N_{A,D} + \Delta n}{qWn_i^2}\right) + \frac{1}{\tau_{\text{bulk}}}. \quad (2)$$

In practice, we find that (2) is effective for evaluating J_{0e} and τ_{bulk} even at moderate injection levels ($\Delta n \geq N_{A,D}$). For modern cells, the historical recommendation [11] to apply this method only to high-injection conditions ($\Delta n \geq 10 \times N_{A,D}$) is unnecessarily restrictive, perhaps due to the reduced injection-dependence of τ_{bulk} seen in modern n-type substrates and Ga-doped p-type substrates. Fig. 1 shows τ_{bulk} versus carrier

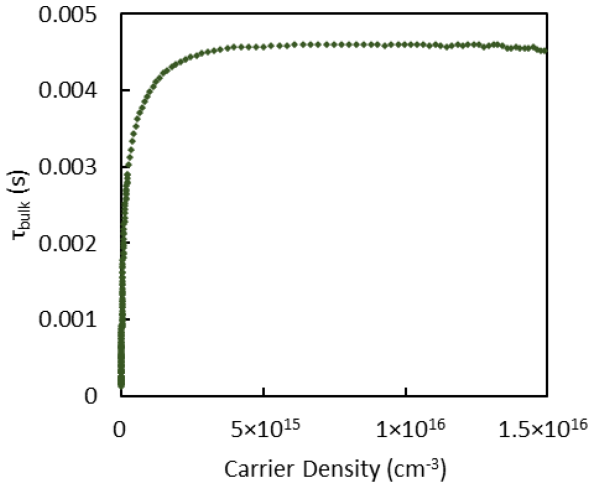

Fig. 1. Injection dependence of the bulk lifetime for an industrial TOPCon solar cell.

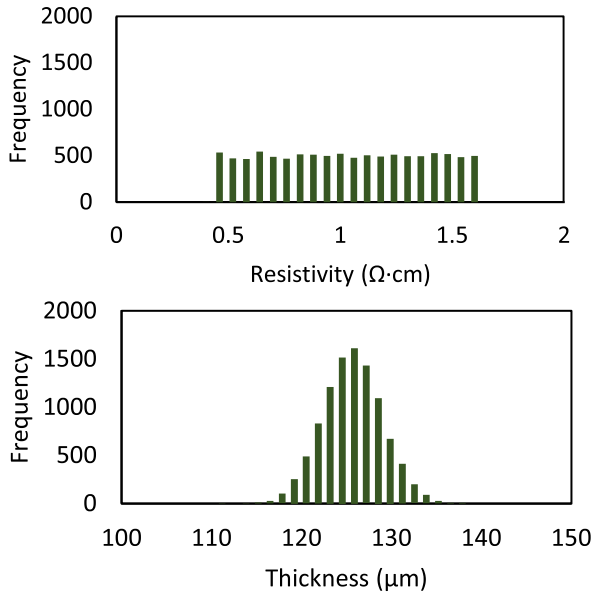

Fig. 2. Input distributions of substrate resistivity and thickness.

density data for an industrial TOPCon solar cell with a doping of 4.6×10^{15} cm^{-3}. True high injection for this cell corresponds to carrier densities greater than 4.6×10^{16} cm^{-3}; however, we can see injection independence of the bulk lifetime for carrier densities at and above the doping level.

Similar to (1), (2) depends directly on substrate doping and thickness. It is also dependent on these input parameters through the model chosen to calculate the Auger correction [13], [14]. For this study, we use the Niewelt et al. model [13], which adds further complex dependencies on the inputs. This model utilizes thickness in the photon recycling calculation and doping in both the *np*-product calculation and the bandgap narrowing calculation [15], [16] which affects the n_i. It should be noted that there is a $\pm$20% uncertainty in the analysis for the Auger model selected here [13].

The J_{0e} and τ_{bulk} parameters measured at the cell level can be utilized along with the measured series resistance (R_s) and measured shunt resistance (R_{sh}) to perform a power loss analysis of the cell [1]. This analysis provides insight into the dominant loss mechanisms affecting device performance. Accurately identifying these mechanisms is crucial for implementing targeted process improvements, ensuring that corrective actions address the most significant contributors to efficiency losses.

Due to the complex dependencies of the reported carrier recombination lifetime parameters on resistivity and thickness, Monte–Carlo methods are the most reasonable way to assess the sensitivities of these results due to the inputs.

II. Method

For industrial relevance, 50 TOPCon solar cells were measured and analyzed using the Sinton Instruments FCT-650, which measures *I*–*V* curves, Suns-Voc curves, and substrate doping [17] to perform carrier recombination lifetime analyses. The J_{0e} values for these samples ranged from 3 to 60 fA/cm^2 and the τ_{bulk} values ranged from 800 to 13000 μs. Half of the samples were nominally 125 μm thick and half were nominally 150 μm thick. Their substrate resistivities ranged from 0.55 to 1.4 Ω·cm. Overall, the range of values makes this a diverse sample set to analyze.

The measurement data from the FCT-650 were used in a Monte–Carlo sensitivity analysis where realistic production distributions (see Fig. 2) of input resistivity and thickness were randomly generated. The resistivities and thicknesses from these distributions were paired at random and used as inputs for the carrier recombination lifetime analysis of the FCT-650. Corresponding output distributions of τ_{eff} at the maximum power point ($\tau_{\text{eff@Vmp}}$), J_{0e}, and τ_{bulk}, as well as full injection-dependent lifetime curves were generated. The input distributions (see Fig. 2) were generated as follows.

1) *Resistivity input*: Uniform distribution spanning 0.4–1.6 Ω·cm [3]. While this uniform distribution simplifies the resistivity profile compared to actual production distributions where variations might be more complex or skewed, the choice of this distribution simplifies modeling while retaining the full possible range of resistivities. In addition, with advances in growth processes, the distribution in resistivity is technology-dependent [18]. In production, this could be quickly evaluated for large numbers of incoming wafers from a known vendor. For the limited data shown in this article and available in our facility, the distributions in resistivity did not follow any recognizable pattern justifying any specific assumption.
2) *Thickness input*: Normal distributions centered around 125 (samples 1–25) and 150 μm (samples 26–50) with $\pm 3\sigma$ corresponding to ± 10 μm [4]. This range was selected as a midrange point per various specification sheets [3], [4], [5].

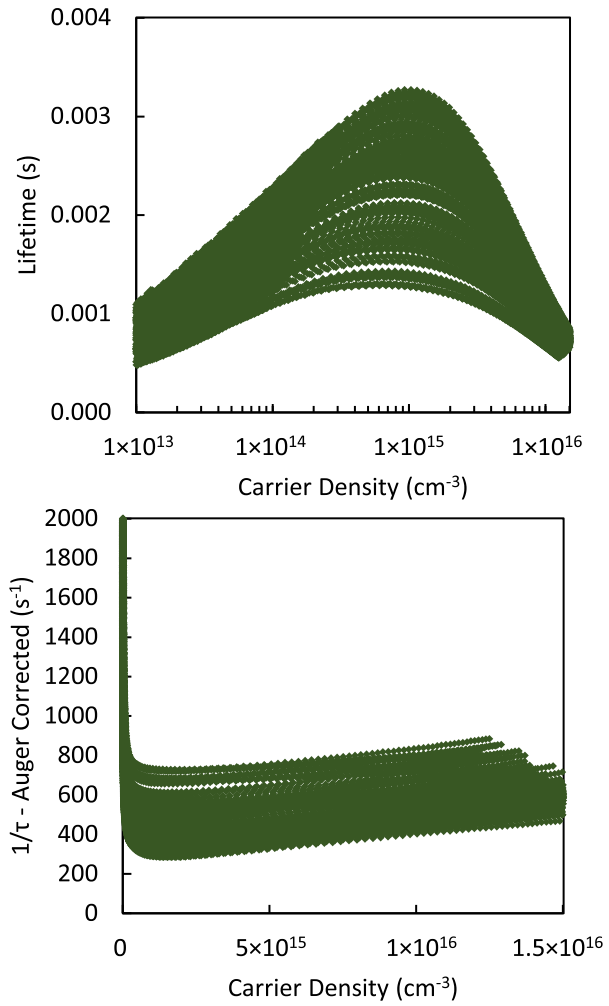

Fig. 3. Injection dependent lifetime curves resulting from varying both the input resistivity and thickness.

TABLE I
MEAN VALUES AND 95% CIS FOR THE CARRIER RECOMBINATION LIFETIME RESULTS FOR SAMPLE 29 WHEN VARYING THE INPUT RESISTIVITY AND THICKNESS

Result	Mean	95% CI
J_{0e} (fA/cm^2)	3.31	1.95– 4.20 (-41.2% to 26.7%)
τ_{bulk} (μs)	4573	1989–6673 (-56.5% to 45.9%)
$\tau_{eff@Vmp}$ (μs)	2161	1302–2738 (-39.7% to 26.7%)

III. RESULTS AND DISCUSSION

Fig. 3 shows the resulting injection-dependent lifetime and inverse lifetime curves for a single sample (sample 29) when the input distributions of substrate resistivity and thickness are fed into the analysis. There is a large uncertainty in the lifetime curves due to the uncertainty in the inputs, which trickles down to many of the measured lifetime parameters, including $\tau_{\mathrm{eff@Vmp}}$, J_{0e}, τ_{bulk}, and additional power loss analysis metrics. Table I reports the mean values and 95% confidence intervals (CI) for the output distributions. We see fairly wide CIs for the case where both the input thickness and resistivity are varied in the analysis. The resulting J_{0e} distribution has a 95% CI spanning 2.3 fA/cm^2, and the τ_{bulk} distribution has a 95% CI spanning 4695 μs. This clearly falls short of the goal of reporting J_{0e} with uncertainties less than 1 fA/cm^2. Further improvement is obviously necessary for reliable and accurate carrier recombination lifetime analyses.

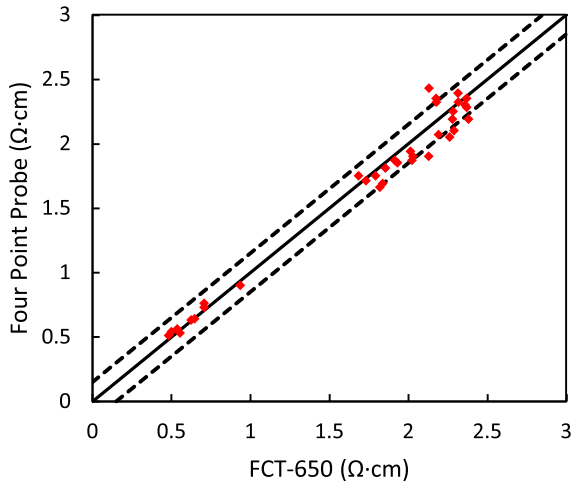

Fig. 4. Agreement between four-point-probe measured wafer resistivity and FCT-650 measured resistivity. Solid black line represents Y = X; dotted black lines represent ±0.15 Ω·cm.

Any reduction in input parameter uncertainty will allow for less uncertainty in the carrier recombination lifetime measurement results. At the cell level, the substrate doping and thickness can be measured with various methods. These parameters can be measured at the wafer stage and tracked through the cell processing steps [19]. Alternatively, cell thickness can be measured at the cell level by weighing the cells.

For this study we will utilize the cell resistivity and thickness measurements available on the FCT-650 test instrument [17]. In solar cells operating between the maximum power point and open-circuit voltage, excess minority carriers introduce time-dependent behavior in current and voltage measurements—often described as a capacitance effect [20], [21]. By solving for self-consistency across data collected under varying conditions of time-varying illumination, current, and voltage, it becomes evident that the measured current and voltage only reflect true steady-state values when the capacitance corrections are applied using the correct doping level. This enables a unique determination of the material's resistivity. Using this method, the FCT-650 can provide a substrate doping measurement for all samples, and in many cases a thickness measurement when high-injection data are available. Such data are available for 36 of the 50 TOPCon cells studied. High-injection data are often not available on lower lifetime cells or samples that are heavily doped. There is uncertainty in the measured resistivity from the FCT-650. This uncertainty is a combination of uncertainty in the input thickness and systematic uncertainty. From a previous study of the FCT-650 doping measurement using a sample set spanning 0.5–2.5 Ω·cm samples, the wafers were measured via four-point probe prior to processing and then made into cells while tracking the initial resistivity value. Fig. 4 demonstrates the agreement between the four-point probe resistivity value and the FCT-650 measured resistivity value. For samples in

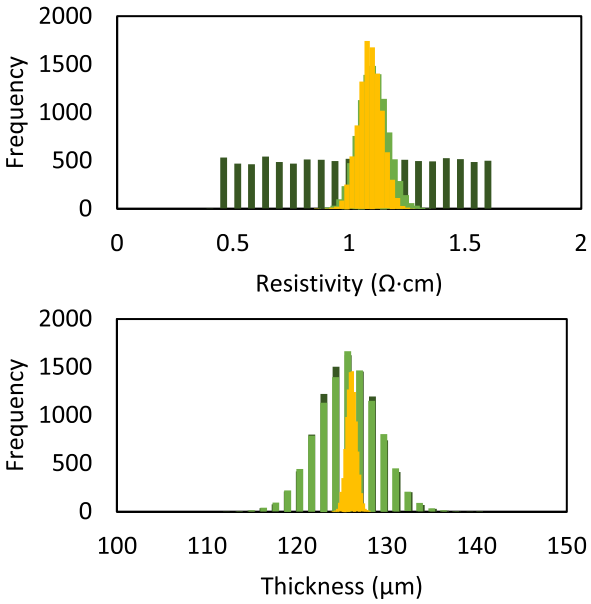

Fig. 5. Uncertainty in measured resistivity (light green), measured resistivity and thickness (yellow) versus. Wafer specification sheet range (dark green).

the resistivity range of interest, we see very good agreement between the two values giving a measured resistivity uncertainty of ± 0.15 Ω·cm that we will consider for further Monte–Carlo simulations.

New input distributions can be generated for two cases of reducing the input parameter uncertainty. The first case will be the reduction of uncertainty when using the measured resistivity value while keeping the same uncertainty in the input thickness. These distributions are shown in light green in Fig. 5. The second case is the reduction in uncertainty in both input parameters using the measured resistivity and measured thickness, as shown in yellow. The uncertainty in the measured thickness is found to be about ± 2 μm for this method. These cases are in contrast with the original wafer specification sheet distributions, as shown in dark green.

Using the tighter distribution for substrate resistivity, and for both resistivity and thickness, we obtain the injection dependent lifetime curves shown in Fig. 6 as well as the output distributions of J_{0e} and τ_{bulk} found in Fig. 7. In Fig. 6, we see a significant reduction in the uncertainty of the injection-dependent lifetime curves. This reduction in uncertainty trickles down to specific lifetime parameters of interest reported in Fig. 7. When looking at the Auger-corrected inverse lifetime curves in Fig. 6, we see that the uncertainty in thickness when using the measured resistivity (light green) contributes most to the uncertainty in the slope of this curve with a fan-like appearance on this light green data with the larger slopes (and thus larger J_{0e}) resulting from thinner thickness inputs. The fan-like appearance goes away when reducing the input thickness uncertainty and utilizing the measured thickness and resistivity in the analysis as seen with the yellow data points.

In Fig. 7, we see the asymmetry of the output J_{0e}, τ_{bulk}, and $\tau_{@\text{Vmp}}$ due to the logarithmic dependence on substrate doping. This logarithmic dependence is much less pronounced

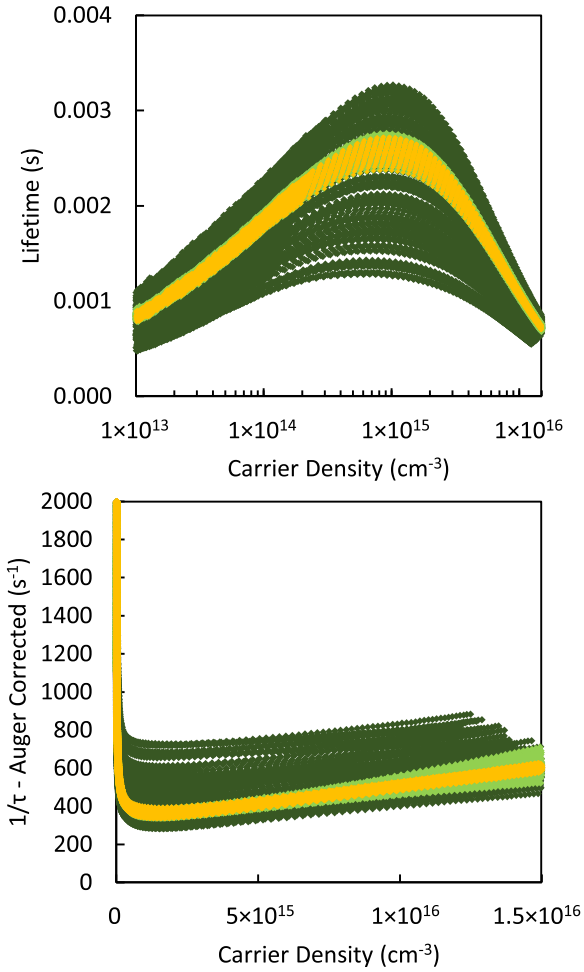

Fig. 6. Injection-dependent lifetime curves generated with the tighter input distributions from the measured values.

with the use of the narrower distribution of measured resistivity and thickness though it is still present and results in asymmetric 95% CIs.

Table II summarizes the reduction in the 95% CIs when using the measured resistivity and thickness distributions rather than the original distributions from the wafer specification sheet. With the measured resistivity as an input, we can achieve a J_{0e} measurement with less than 1 fA/cm^2 uncertainty for this 3.31 fA/cm^2 sample and less than 0.15 fA/cm^2 uncertainty when using the measured resistivity and thickness. In addition, we see a large reduction in the τ_{bulk} uncertainty reducing the 95% CI from -2587, $+2106$ to -361, $+337$ μs for this 4992 μs sample.

J_{0e} and τ_{bulk} are commonly used in power loss analyses. The FCT-650 generates power loss curves showing the power versus voltage for each loss mechanism along with the Auger limit curve. Fig. 8 shows these graphs and their uncertainties in the Suns-Voc curve (red), Auger limit curve (black), Auger + bulk recombination curve (grey), and Auger + emitter curve (blue). The left of Fig. 8 represents uncertainties from varying input thickness and resistivity while the right represents uncertainties from using the measured resistivity and thickness. The reduced

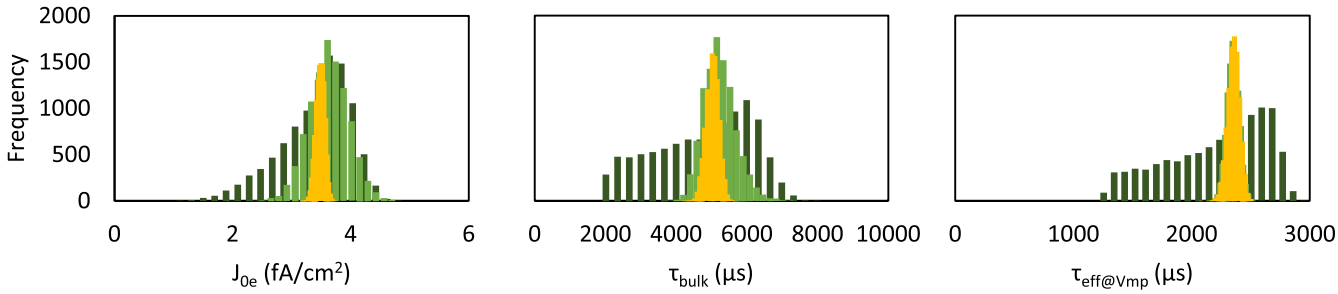

Fig. 7. Output distributions of J_{0e} , τ_{bulk}, and $\tau_{\mathrm{eff@Vmp}}$.

TABLE II
MEAN VALUES AND 95% CIS FOR THE CARRIER RECOMBINATION LIFETIME RESULTS DUE TO DIFFERENT INPUT DISTRIBUTIONS OF RESISTIVITY AND THICKNESS

	Vary Both Inputs (■)		Measured Resistivity (■)		Measured Resistivity and Thickness (■)	
Result	Mean	95% CI	Mean	95% CI	Mean	95% CI
J_{0e} **(fA/cm²)**	3.31	1.95–4.20 (-41.2% to 26.7%)	3.56	2.92–4.21 (-18.2% to 18.1%)	3.47	3.33–3.60 (-4.06% to 3.73%)
τ_{bulk} **(μs)**	4573	1989–6673 (-56.5% to 45.9%)	5131	4340–6115 (-15.4% to 19.2%)	4992	4631–5329 (-7.23% to 6.75%)
$\tau_{\mathrm{eff@Vmp}}$ **(μs)**	2161	1302–2738 (-39.7% to 26.7%)	2339	2236–2438 (-4.39% to 4.23%)	2344	2241–2440 (-4.40% to 4.06%)

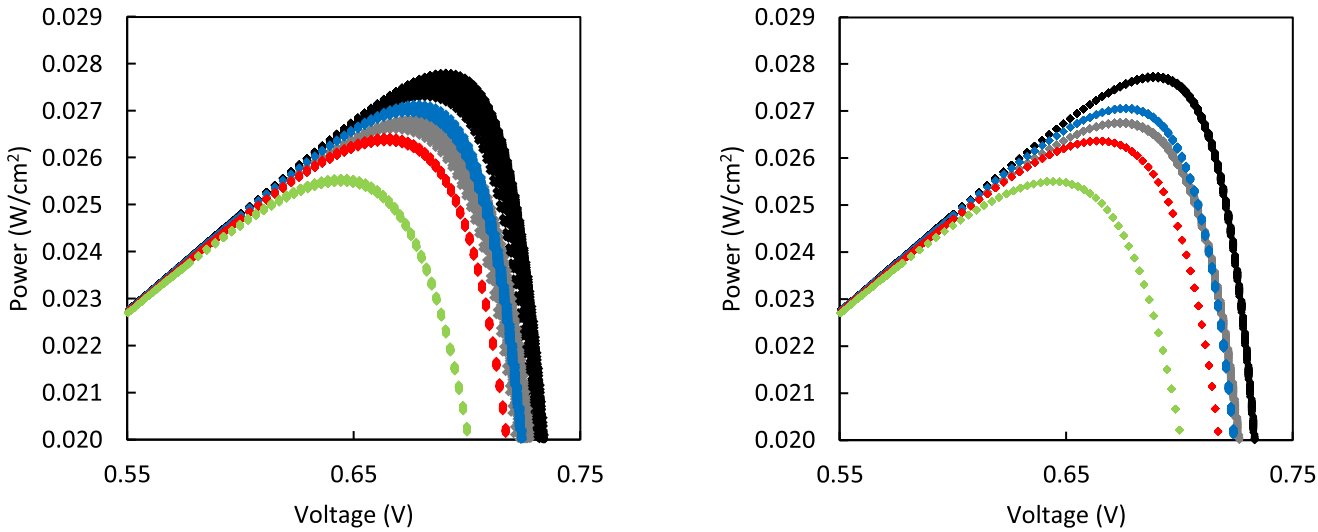

Fig. 8. Power loss analysis curves with varied thickness and resistivity (left) and reduced uncertainty in the inputs (right). The *I–V* curve is green, Suns-Voc curve is red, Auger limit curve is black, Auger + bulk recombination curve is grey, and Auger + emitter curve is blue.

uncertainty in these power loss metrics allows for better process control and optimization with more concrete knowledge of the dominant loss mechanism.

Fig. 9 shows the 95% CIs for J_{0e} and τ_{bulk} for all 50 TOPCon samples studied when varying both the input thickness and resistivity (dark green), when varying only thickness and utilizing the measured resistivity in the analysis (light green), and when utilizing the measured resistivity and thickness when available (yellow). In all cases, we see a drastic reduction in uncertainty of the J_{0e} and τ_{bulk} results when utilizing the measured values of the inputs in the analysis. Sample 2 demonstrates some cases of nonphysical, negative J_{0e} values that are eliminated when using the measured resistivity in the analysis. For samples 1 through 14 using the measured resistivity in the analysis, we see on average a 64% reduction in the 95% CI for J_{0e} and a 75% reduction in the 95% CI for τ_{bulk}. For samples 15 through 50, utilizing the measured resistivity and thickness in the analysis, we see an 87% and 85% reduction in the 95% CIs for J_{0e} and τ_{bulk}, respectively.

An interesting trend that we see is less uncertainty in J_{0e} with higher bulk lifetimes. This is due to the injection independence of the high bulk lifetime samples leading to less uncertainty in the J_{0e}. Fig. 10 demonstrates this uncertainty trend. Even when varying both inputs, we see below ± 1 fA/cm^2 uncertainty for

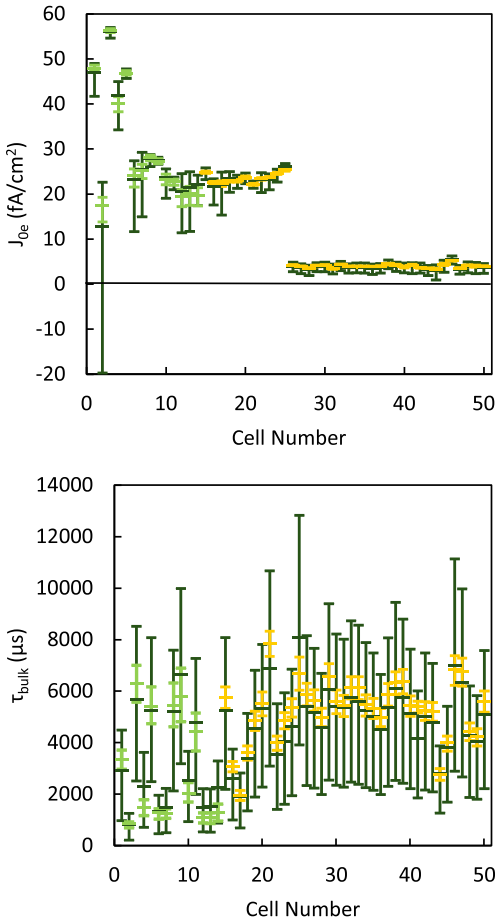

Fig. 9. 95% CI for 25 samples when varying both inputs (dark green), when using measured resistivity with varied thickness (light green), and when using measured resistivity and thickness (yellow).

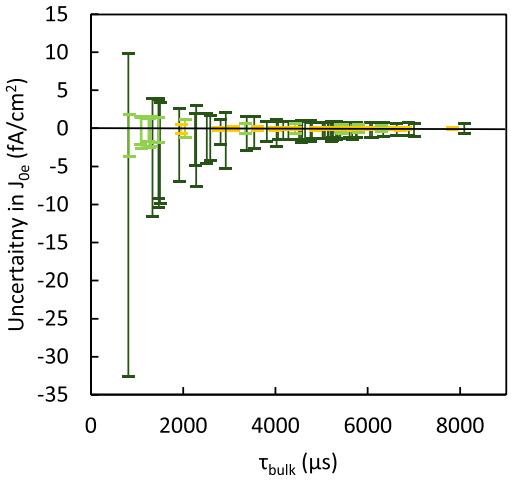

Fig. 10. Uncertainty in J_{0e} versus τ_{bulk}.

bulk lifetimes greater than 6500 μs. When using the measured values as inputs to the analysis, all but eight of these samples have less than ± 1 fA/cm^2 uncertainty in J_{0e}. The six samples with larger uncertainty are samples 2, 4, 6, 7, 10, 12, 13, and 14. These samples also exhibit the smallest bulk lifetimes, all less than 2100 μs.

IV. Conclusion

Carrier recombination lifetime measurements are essential at the cell level to assess the dominant mechanisms of power loss and indicate potential areas for process optimization. These measurements are sensitive to the input parameters of thickness and resistivity. Knowledge of the input parameters beyond what a wafer specification sheet indicates is essential in achieving less than 1 fA/cm^2 uncertainty in the measured J_{0e}. When both the thickness and resistivity are measured and known with greater accuracy than what is given on the wafer specification sheet, very accurate carrier lifetime measurements are achieved. In this case, J_{0e} is known on average to within ± 0.18 fA/cm^2 for samples with J_{0e} values less than 10 fA/cm^2 and τ_{bulk} known on average to within ± 400 μs for samples with lifetimes ranging from 2000 to 8000 μs.

References

[1] H. Wilterdink, R. Sinton, C. Sainsbury, J. Dinger, and W. Dobson, *Power Loss Analysis Based On Device Physics For Photovoltaic Solar Cells and Modules*. Breckenridge, CO, USA: NREL Silicon Workshop, 2025.

[2] C. Ballif, F. J. Haug, M. Boccard, P. J. Verlinden, and G. Hahn, "Status and perspectives of crystalline silicon photovoltaics in research and industry," *Nature Rev. Mater.*, vol. 7, pp. 597–616, 2022.

[3] Longi, "Monocrystalline wafer specification, N-type-M10-Res0.4∼1.6-A grade," (n.d.). [Online]. Available: https://static.longi.com/Monocrystalline_Wafer_N_type_M10_Res0_4_1_6_A_Grade_cb59990f3c.pdf

[4] Longi, "Monocrystalline wafer specification, P-type-M10-Res0.4∼1.1-A grade," (n.d.). [Online]. Available: https://static.longi.com/Monocrystalline_Wafer_P_type_M10_Res0_4_1_1_A_Grade_708e023634.pdf

[5] Norsun, "Our products," (n.d.). [Online]. Available: https://www.norsun.no/products

[6] A. L. Blum, H. W. Wilterdink, and R. A. Sinton, "Sensitivity analysis of Eddy current excess carrier recombination lifetime measurements due to input parameter uncertainty," *IEEE J. Photovolt.*, vol. 15, no. 3, pp. 393–399, May 2025, doi: 10.1109/JPHOTOV.2025.3539294.

[7] K. McIntosh and R. A. Sinton, "Uncertainty in photoconductance lifetime measurements that use an inductive-coil detector," in *Proc. 23rd Eur. Photovolt. Sol. Energy Conf. Exhib.*, Valencia, Spain, 2008, pp. 77–82.

[8] A. F. Thomson et al., "Uncertainty in photoconductance measurements of the emitter saturation current," *IEEE J. Photovolt.*, vol. 3, no. 4, pp. 1200–1207, Oct. 2013, doi: 10.1109/JPHOTOV.2013.2270346.

[9] R. A. Sinton and A. Cuevas, "A quasi-steady-state open-circuit voltage method for solar cell characterization," in *Proc. 16th Eur. PVSEC*, 2000, pp. 1–4.

[10] A. L. Blum, R. A. Sinton, W. Dobson, H. Wilterdink, and J. H. Dinger, "Lifetime and substrate doping measurements of solar cells and application to in-line process control," in *Proc. IEEE 43rd Photovolt. Specialists Conf.*, Portland, OR, USA, 2016, pp. 3534–3537.

[11] D. E. Kane and R. M. Swanson, "Measurement of the emitter saturation current by a contactless decay method," in *Proc. 18th IEEE Photovolt. Specialists Conf.*, 1985, pp. 578–583.

[12] K. Dapprich et al., "Generalizing axis choice for fitting surface recombination current in light of band gap narrowing for silicon photovoltaics," *AIP Conf. Proc.*, vol. 2826, no. 1, Jun. 2023, Art. no. 030004.

[13] T. Niewelt et al., "Reassessment of the intrinsic bulk recombination in crystalline silicon," *Sol. Energy Mater. Sol. Cells*, vol. 235, 2022, Art. no. 111467.

[14] R. A. Sinton and R. M. Swanson, "Recombination in highly injected silicon," *IEEE Trans. Electron Devices*, vol. ED-34, no. 6, pp. 1380–1389, Jun. 1987.

[15] A. Schenk, "Finite-temperature full random-phase approximation model of band gap narrowing for silicon device simulation," *J. Appl. Phys.*, vol. 84, no. 7, pp. 3684–3695, 1998.

[16] P. P. Altermatt, A. Schenk, F. Geelhaar, and G. Heiser, "Reassessment of the intrinsic carrier density in crystalline silicon in view of band-gap narrowing," *J. Appl. Phys.*, vol. 93, no. 3, pp. 1598–1604, 2003.

[17] R. A. Sinton, M. K. Forsyth, A. L. Blum, and J. S. Swirhun, "Characterization of substrate doping and series resistance during solar cell efficiency measurement," US Patent 10,027,278 B2, Jul. 17, 2018.

[18] Longi, "LONGi brings next generation TaiRay silicon wafer products to the global PV market," Apr. 28, 2024. [Online]. Available: https://www.longi.com/en/news/silicon-new-product-release/

[19] S. Wanka et al., "Tra.Q — Laser marking for single wafer identification — Production experience from 100 million wafers," in *Proc. 37th IEEE Photovolt. Specialists Conf.*, Seattle, WA, USA, 2011, pp. 001101–001104, doi: 10.1109/PVSC.2011.6186144.

[20] R. A. Sinton, H. W. Wilterdink, and A. L. Blum, "Assessing transient measurement errors for high-efficiency silicon solar cells and modules," *IEEE J. Photovolt.*, vol. 7, no. 6, pp. 1591–1595, Nov. 2017.

[21] A. L. Blum, R. A. Sinton, and H. W. Wilterdink, "Determining the accuracy of solar cell and module measurements on high-capacitance devices," in *Proc. 2018 IEEE 7th World Conf. Photovolt. Energy Convers.*, Waikoloa, HI, USA, 2018, pp. 3603–3606, doi: 10.1109/PVSC.2018.8548016.